

# Feasibility Studies on a Downstream Injection System for Mu2e Calorimeter Calibration Electrons

Guangyong Koh<sup>a</sup>, John Alsterda<sup>a</sup>, Grace Bluhm<sup>a,c</sup>, George Gollin<sup>a,\*</sup>, Tim He<sup>a</sup>, Matthew McHugh<sup>a</sup>, Daniel Pershey<sup>a,b</sup>

<sup>a</sup>Department of Physics, University of Illinois at Urbana-Champaign

<sup>b</sup>Department of Physics, Harvard University

<sup>c</sup>Department of Physics, University of Wisconsin-Whitewater

August 7, 2009

## Abstract

A calibration-electron injection system sited downstream of the calorimeters within the Mu2e detector solenoid is expected to be able to simulate electrons captured by the upstream magnetic bottle while being sited away from where the real physics of the experiment is taking place. As a preliminary to more rigorous testing, particle-trajectory simulation using a 4<sup>th</sup>-order Runge-Kutta method in MATLAB was utilized to examine the feasibility of such an injection method. From these studies, it was determined that electron injection through a low-field or field-free annulus around a beam dump presents the most suitable means of populating the phase-space at the tracking vanes for calorimeter calibration purposes.

## Theoretical Considerations Arising From the Magnetic Bottle Configuration

The proposed Mu2e detector solenoid utilizes a magnetic bottle in the vicinity of the stopping targets to capture and redirect upstream-moving electrons from muon capture and muon decay. In particular, the existing proposal (based on MECO specifications) calls for the magnetic field strength in the detector solenoid to decrease from 2 T to 1 T (both directed along the beam axis), progressing downstream over the extent of the stopping target array.<sup>1</sup>

In a magnetic bottle, only particles obeying the inequality

$$\frac{v_{\parallel}}{v_{\perp}} < \sqrt{\frac{B_{\max}}{B_{\min}} - 1} \quad [1]$$

---

\* Contact person: George Gollin, [g-gollin@illinois.edu](mailto:g-gollin@illinois.edu), +1 (217) 333-4451.

where  $\parallel$  ( $\perp$ ) represents the direction parallel (perpendicular) to the magnetic field, will be captured and redirected by the magnetic bottle. Thus, with the proposed magnetic field configuration in the detector solenoid,

$$\frac{v_{\parallel}}{v_{\perp}} < 1 \Rightarrow \frac{v \cos \theta}{v \sin \theta} < 1 \Rightarrow \theta > 45^{\circ} \quad [2]$$

where beam axis has been defined to be the z-axis. Consequently, only electrons with a pitch angle  $\theta > 45^{\circ}$  with respect to the magnetic field in the detector solenoid will be captured by the magnetic bottle.

The proposed injection of calibration-electrons downstream of the calorimeters in the detector solenoid intends to take advantage of the above-mentioned magnetic bottle to simulate helical electron trajectories emitted from the stopping targets. For this to occur, Eqn. 2 must be obeyed.

#### *Adiabatic Invariance of the Magnetic Moment*

A constraint on design parameters for any electron injector is the adiabatic invariance of a particle's magnetic moment  $\mu$ :

$$\mu = \frac{mv_{\perp}^2}{2B} \quad [3]$$

Thus,

$$\frac{mv^2 \sin^2 \theta_{inj}}{2B_{inj}} = \frac{mv^2 \sin^2 \theta_{det}}{2B_{det}} \quad [4]$$

Since  $\sin^2 \theta_{inj} \leq 1$ ,

$$\sin^2 \theta_{det} \leq \frac{B_{det}}{B_{inj}} \quad [5]$$

Considering Eqn. 1.2, then,

$$\frac{1}{2} < \sin^2 \theta_{det} \leq \frac{B_{det}}{B_{inj}} \quad [6]$$

Consequently, for injected electrons to be captured by the magnetic bottle, the magnetic field in the injector solenoid  $B_{inj}$  cannot be stronger than 2 T (i.e., the strength of the upstream field).

## Method

All simulations presented in this report were done with MATLAB; in particular, magnetic fields were simulated and mapped using numerical Biot-Savart integrations, and particle trajectories were simulated using a 4<sup>th</sup>-order Runge-Kutta method. Simulations were conducted with the upstream-most stopping target centered on the origin and the z-axis pointing downstream along the beam-line; the positive x- and y- axes were beam- left and up respectively (when viewed from upstream). In addition to that of calibration electrons, trajectories of positrons were simulated as well, as a means of determining the injection conditions required for the attainment of particular phase-space states at various positions within the detector solenoid (e.g., at the stopping targets).

## Findings

### *With a 5 T Injection Field*

It should be noted that since  $\mu$  is an adiabatic rather than an absolute invariant, the possibility exists that certain parameters can be manipulated to promote its non-conservation. In particular, for the adiabatic assumption to hold, the field strength has to be varying spatially on length scales much greater than the Larmor radius of the spiraling electron.<sup>2</sup>

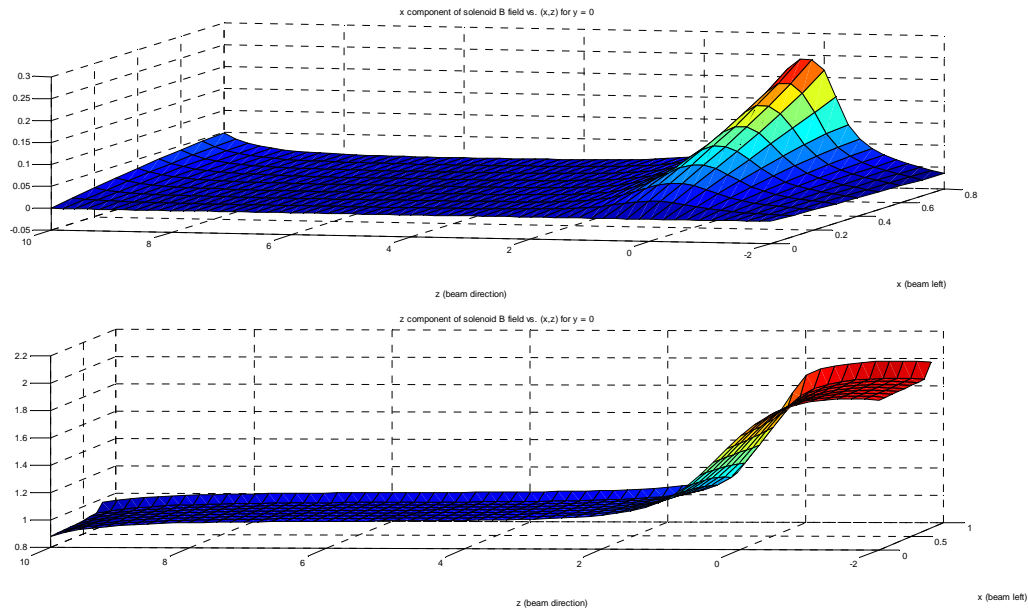


**Figure 1.** Simulated mapping of the magnetic field strength in the detector solenoid in the range  $z = -2$  m to  $z = 10$  m. The field map indicates that the field strength ramps from 1 T to 2 T over a distance of  $\sim 2$  m.

Based on a simulated mapping of the magnetic field within the detector solenoid (for the range  $-2$  m to  $10$  m), it was determined that the field strength ramped from 1 T to 2 T over a distance of  $\sim 2$  m (Fig. 1). With this mapping of the magnetic field, the trajectory of a 105 MeV/c electron within the detector solenoid was simulated; in particular, a Larmor radius of  $\sim 0.25$  m was

observed when the electron was injected directly into the detector solenoid with  $\theta = 135^\circ$ . Comparing this simulated Larmor radius with the expected (i.e., calculated) Larmor radius of

$$r = \frac{\gamma m v_{\perp}}{|q| B} = 2.477 \quad [7]$$

where  $\gamma$  is the Lorentz factor, it can be seen that the simulated mechanics are in close correlation with the real physics.

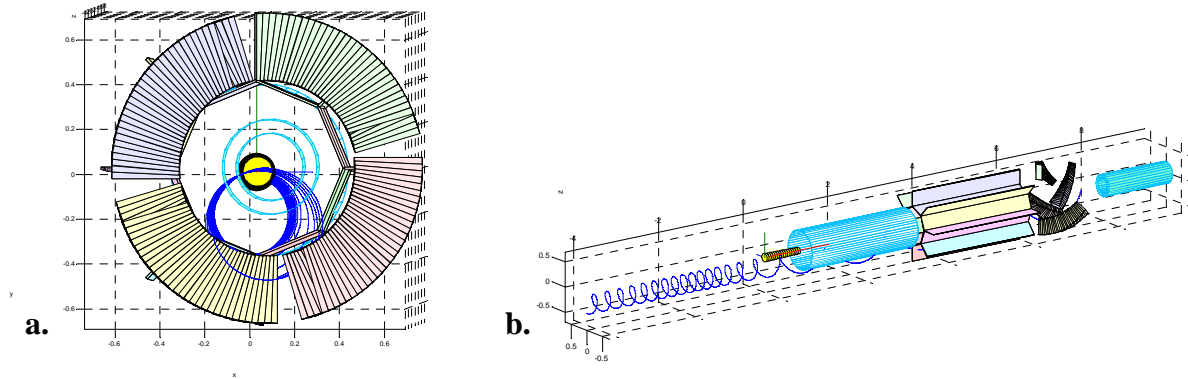


**Figure 2a.** End-on, and **b.** isometric profile of a simulated electron trajectory, beginning in the detector solenoid itself at  $z = 7.5$  m (i.e., downstream of the calorimeters), with a pitch angle  $\theta = 135^\circ$ . Of note is the Larmor radius of  $\sim 0.25$  m, which corresponds well with the theoretical value of 2.477 m.

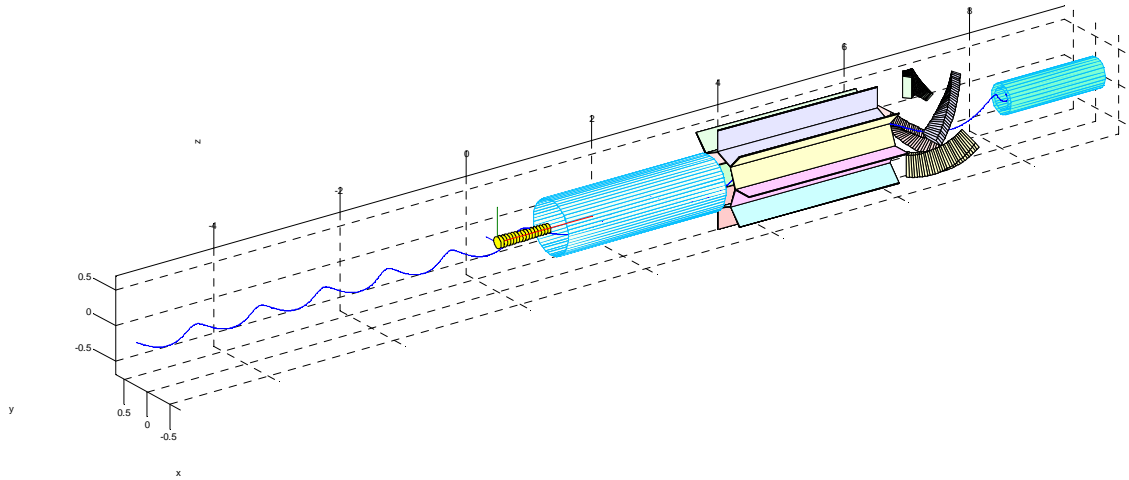


**Figure 3.** Isometric profile of a simulated electron trajectory injected with  $z = 8.75$  m,  $\theta = 91^\circ$ , in the 5 T field of the injector solenoid. Despite the high  $\theta$ , the injected electron is not captured by the magnetic bottle at the upstream end of the detector solenoid.

Comparison of the simulated Larmor radius and field-ramping length scales suggests that the adiabatic approximation may not be strong enough for the adiabatic invariant to hold. However, simulations of the trajectories of electrons injected through a 5 T solenoid into the downstream

end of the detector solenoid showed that injected electrons would not be captured by the magnetic bottle, even with initial pitch angles as high as  $91^\circ$  (Fig. 3). It can thus be concluded that a 5 T injector solenoid is unfeasible under the current specifications for the detector solenoid.

*With a 2 T Injection Field*

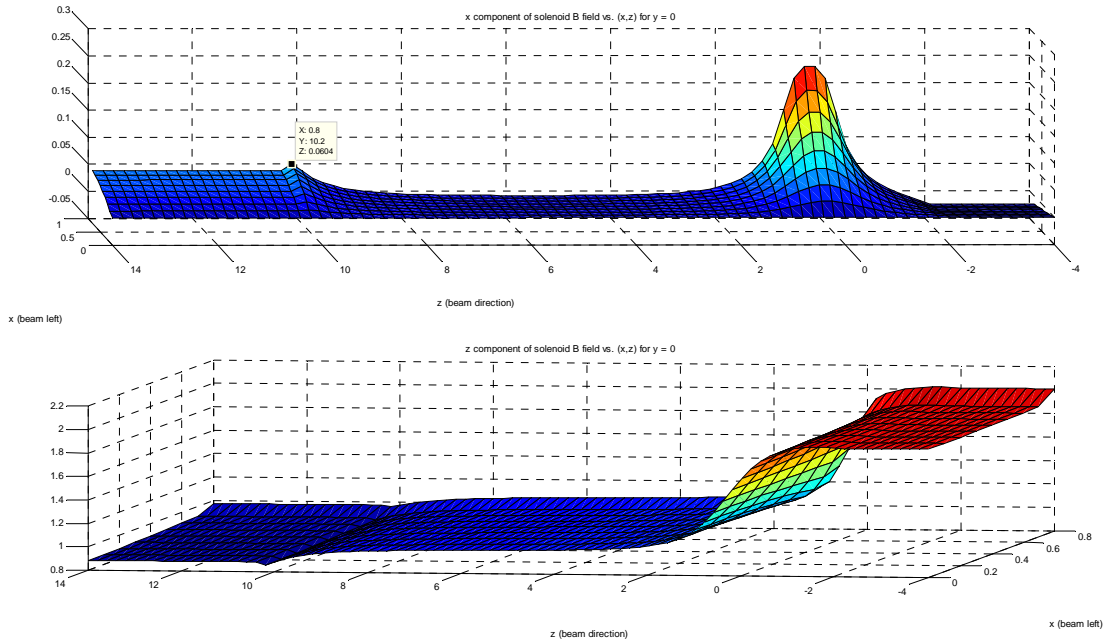


**Figure 4.** Simulated mapping of the magnetic field strength in the detector solenoid in the range  $z = -4$  m to  $z = 14$  m.

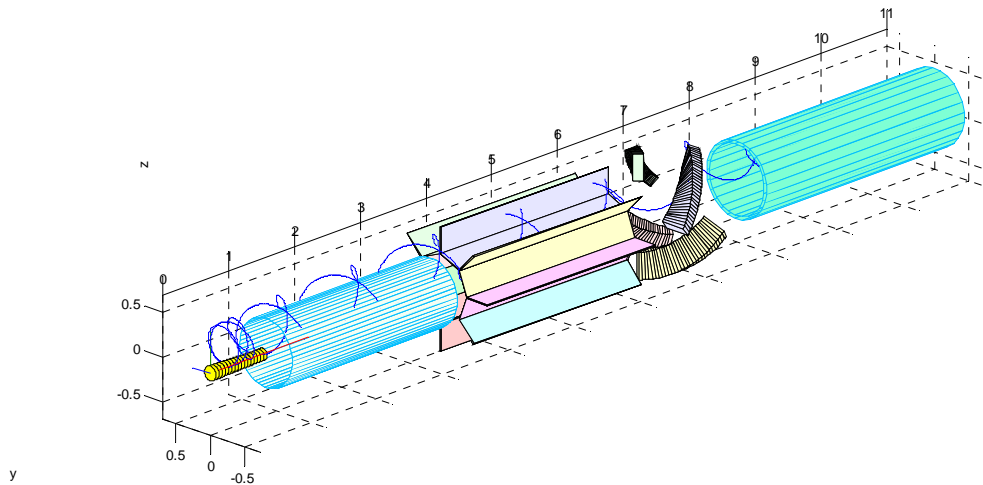


**Figure 5.** Isometric profile of a simulated electron trajectory injected with  $z = 9$  m,  $\theta = 110^\circ$ , in the 2 T field of the injector solenoid. The electron is captured by the magnetic bottle as desired. However, the size of the injection solenoid required for such a configuration is comparable to that of the tracker, and is consequently impractical.

Based on the consideration of the adiabatic invariance of the calibration electron’s magnetic moment (mentioned above), a new model of the injection solenoid, this time with a net 2 T field—obtained via a superposition of the detector solenoid’s magnetic field and an additional 1 T injector solenoid field—, was examined. In addition, a new mapping of the magnetic field within the detector solenoid was simulated and utilized, this time with an extended mapped range of  $-4\text{ m}$  to  $14\text{ m}$  (Fig. 4).

With the new injector solenoid parameters, it was observed that injected electrons were captured by the magnetic bottle for  $90^\circ < \theta < \sim 110^\circ$  (Fig. 5). However, the injection solenoid itself had to possess an inner radius (i.e., excluding the flux return yoke) of  $\sim 0.4\text{ m}$  in order for injected electrons to cover a significant region of phase-space at the injector outlet. This makes the required size of the injection solenoid comparable to that of the tracker itself, which, coupled with its proposed positioning on the beam axis, renders it impractical in the form presented here.

*With a 0 T Injection Field*

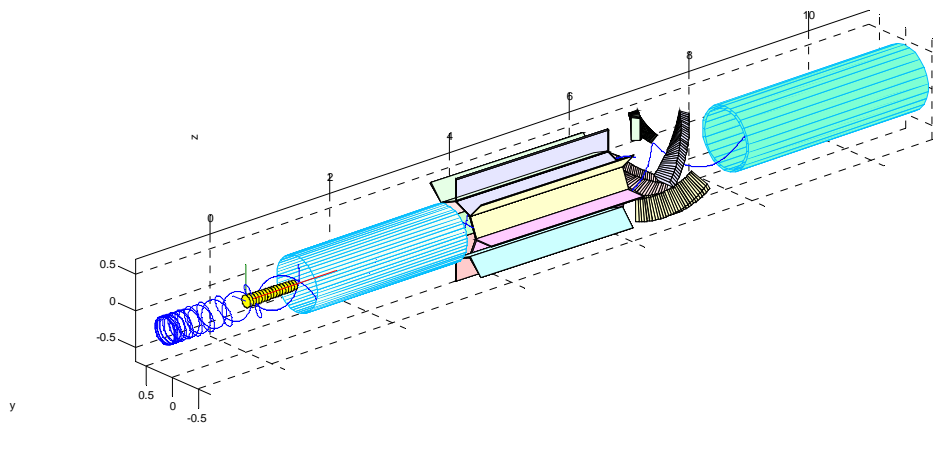


**Figure 6.** Isometric profile of a simulated electron trajectory injected with  $z = 8.4\text{ m}$ ,  $\theta = 145^\circ$ , in the 0 T field of the injector solenoid. The electron is captured by the magnetic bottle as desired.

The polarity of the 1 T injector solenoid field was next reversed to study the effect of employing a field-free injection port (obtained through a superposition of the 1 T detector solenoid field with the now  $-1\text{ T}$  injector solenoid field). This configuration demonstrated good results, with the simulated electrons being captured by the magnetic bottle for  $90^\circ < \theta < \sim 145^\circ$  (Fig. 6)—a marked improvement over both of the previously examined injection field strengths.

*Through a Field-Free Injector into an Annulus around a Beam Dump*

To investigate the viability of injecting test electrons through a field-free injector into an annulus around a beam dump, positron trajectories emerging from the stopping targets were simulated, and their profiles downstream studied. This was conducted with the mapping of the detector solenoid’s magnetic field as seen in Fig. 4—based on a 1 T solenoid whose coils extended to  $z = 11\text{ m}$ , and which did not possess a flux return yoke. The results of these simulations agreed with expectations, in that electrons injected around the beam dump—and hence off the beam axis—would spiral around the radially dispersing magnetic field lines (downstream of the

calorimeters, where the field is weakening), and hence eventually make their way radially inward to the stopping targets (Fig. 7).

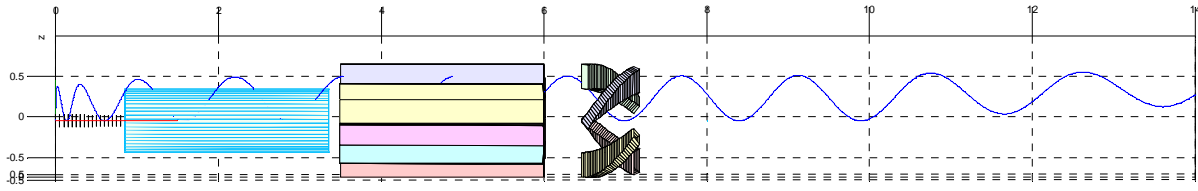


**Figure 7.** Side profile of a simulated electron trajectory eventually passing through the center of the first stopping target with  $\varphi = 0^\circ$  and  $\theta = 90^\circ$ . Of note is the gradual departure of the electron’s gyration axis from the beam axis as the magnetic field weakens in the downstream region of the detector solenoid. This demonstrates the viability of electron injection around the beam dump—especially with the presence of a return yoke, which would cause the magnetic field to ramp down over a much shorter distance.

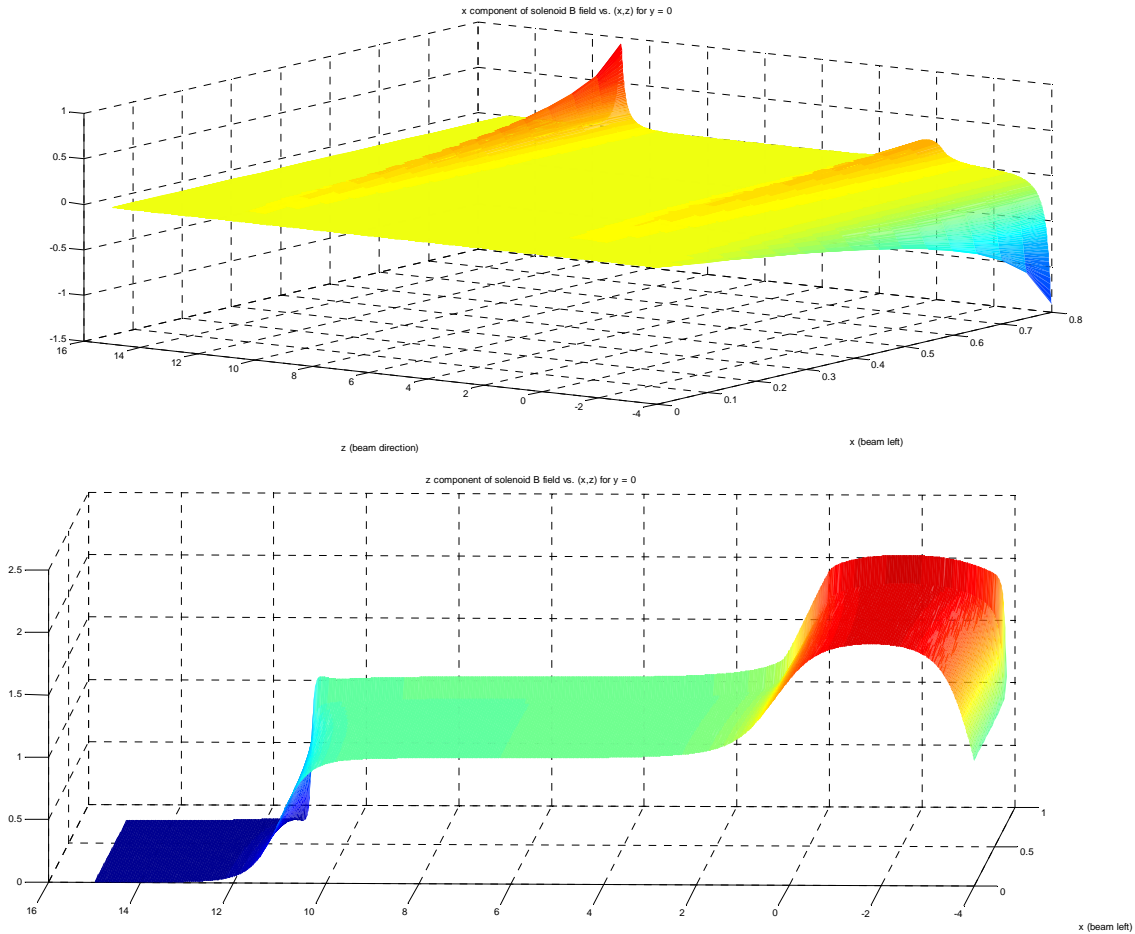


**Figure 8.** Simulated mapping of the magnetic field strength in the detector solenoid in the range  $z = -4$  m to  $z = 15$  m, this time with the additional consideration of a flux return yoke. Of note is the drastic ramping-down of the magnetic field strength at  $z = 11$  m, where the solenoid coils end.

Because of the lack of a flux return yoke, the magnetic field strength downstream weakened very gradually, and was  $\sim 0.895$  T at  $z = 14$  m (Fig. 4). Based on these specifications, the positrons’ (simulating electrons) minimum distance-of-approach to the beam axis in the 12–14 m range was

$\sim 0.15$  m, with a maximum Larmor radius of  $\sim 0.27$  m. As these dimensions will eventually have to work in conjunction with a beam dump, a larger distance-of-approach to the beam axis is desirable; to reduce running costs, it would be preferable as well to achieve optimum distances-of-approach at lower  $z$ -values.

Since both of these concerns were expected to be addressed by the presence of a flux return yoke, further simulations were conducted with a mapping of the solenoid's magnetic field which had the added consideration of the yoke. From Fig. 8, it can be seen that the magnetic field strength tapers off drastically at the end of the detector solenoid at  $z = 11$  m, effectively establishing a field-free region beyond.

The points at which returning electrons passed through the tracking vanes are shown in Fig. 9; these were obtained from electrons injected at  $z = 12.5$  m,  $y = 0.400$  m and  $0.425$  m,  $\varphi = 205\text{--}215^\circ$  (at  $1^\circ$  intervals), and  $\theta = 158\text{--}162^\circ$  (at  $1^\circ$  intervals). From the figure, it can be seen that there is an even distribution of hits along the  $z$ -extent of the tracking vanes; this, coupled with the positioning of any such injectors away from the muon beam line, makes such an injection profile the most suitable candidate among those studied in this report.

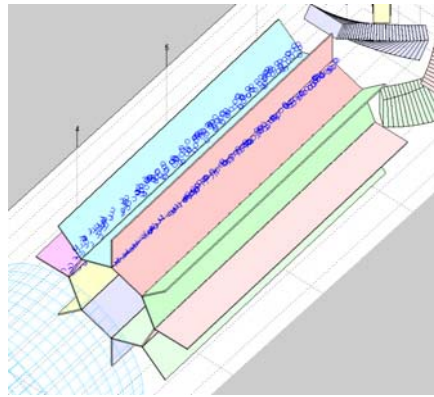


**Figure 9.** Locations at which simulated electron trajectories passed through the tracking vanes; trajectories were simulated for electrons injected at  $z = 12.5$  m,  $y = 0.400$  m and  $0.425$  m, with  $\varphi = 205\text{--}215^\circ$  (at  $1^\circ$  intervals), and  $\theta = 158\text{--}162^\circ$  (at  $1^\circ$  intervals). Of note is the even distribution of hits along the  $z$ (beamline)-extent of the tracking vanes.

## Conclusion

A downstream injection system for Mu2e calorimeter-calibration electrons presents distinct advantages over a more traditional upstream injection system; however, the design parameters for such a system are constrained both by adiabatic invariants such as the electron orbits' magnetic moments, as well as more mundane practical concerns such as size and positioning issues. Of the various downstream injection methods examined in this report, it can be concluded that electron injection through a low-field or field-free region around a beam dump presents the best means of successfully populating the phase-space of interest at the tracking vanes.

<sup>1</sup> Mu2e Collaboration, Proposal to Search for  $\mu^- N \rightarrow e^- N$  with a Single Event Sensitivity Below  $10^{-16}$  (10 Oct. 2008).

<sup>2</sup> A. N. Hall, Astron. Astrophys. **84**, 40-43 (1980).